Spectral sum for the color-Coulomb potential in $SU(3)$ Coulomb gauge lattice Yang-Mills theory

Y. Nakagawa,[1] A. Nakamura,[1] T. Saito,[2] and H. Toki[3]

[1]*Research Institute for Information Science and Education, Hiroshima University, Higashi-Hiroshima, Hiroshima, 739-8521, Japan*
[2]*Integrated Information Center, Kochi University, Kochi, 780-8520, Japan*
[3]*Research Center for Nuclear Physics, Osaka University, Ibaraki, Osaka, 567-0047, Japan*

We discuss the essential role of the low-lying eigenmodes of the Faddeev-Popov (FP) ghost operator on the confining color-Coulomb potential using $SU(3)$ quenched lattice simulations in the Coulomb gauge. The color-Coulomb potential is expressed as a spectral sum of the FP ghost operator and has been explored by partially summing the FP eigenmodes. We take into account the Gribov copy effects that have a great impact on the FP eigenvalues and the color-Coulomb potential. We observe that the lowest eigenvalue vanishes in the thermodynamic limit much faster than that in the Landau gauge. The color-Coulomb potential at large distances is governed by the near-zero FP eigenmodes; in particular, the lowest one accounts for a substantial portion of the color-Coulomb string tension comparable to the Wilson string tension.

PACS numbers: 12.38.Gc, 11.15.Ha, 12.38.Aw
Keywords: lattice QCD, color confinement, Coulomb gauge, Faddeev-Popov ghost operator

I. INTRODUCTION

The use of the Coulomb gauge has great advantages in studying the nonperturbative aspects of Yang-Mills theory, such as color confinement [1–3]. In the Coulomb gauge the three dimensionally transverse components and the time-time component of the gluon propagator do not mix with each other. Although this makes the perturbative calculation cumbersome, the confinement phenomenon can be tackled in a comprehensive way. In QCD gluons play a dual role: confining gluons and confined gluons. Confining gluons mean that the gluons play the role to confine quarks, and they cause a strong long-range correlation between quarks distant apart. Confined gluons indicate that gluons themselves are confined in hadrons, that is, the gauge fields cannot have a correlation beyond the hadronic scale. Such complementary aspects of the gluons can coexist in the Coulomb gauge: The transverse gluon propagator is suppressed in the infrared region, which indicates the confinement of gluons, and the time-time component of the gluon propagator diverges much stronger in the infrared limit than the free field propagator [4–11]. This interpretation of color confinement differs from the confinement mechanism in the covariant gauge, in which the highly random fluctuations of the gauge fields lead the incoherent interference of different paths of the transport of color charges [12].

The Coulomb gauge Hamiltonian contains the instantaneous interaction which plays a significant role in the Gribov-Zwanziger scenario [2]. The instantaneous interaction energy between color charges is called the color-Coulomb potential. Lattice QCD simulations have showed that the color-Coulomb potential rises linearly at large distances and it has $2 \sim 3$ times larger string tension than the static Wilson potential [13–15]. This is consistent with the Zwanziger's inequality which states that the instantaneous color-Coulomb potential provides an upper bound for the static potential [16]. In other words, the necessary condition for the static Wilson potential being a confining potential is that the color-Coulomb potential is also a confining potential. Furthermore, it has been shown that the scaling violation of the color-Coulomb string tension is weaker than that of the Wilson string tension [14, 17].

The confining nature of the color-Coulomb potential is attributed to the accumulation of the low-lying eigenmodes of the Faddeev-Popov (FP) ghost operator. As pointed out by Gribov, the linear gauges such as Coulomb gauge or Landau gauge do not fix the gauge completely [18, 19]. There remain gauge-equivalent configurations after imposing the gauge fixing condition on the gauge fields. In order to select only one representative from each gauge orbit we have to restrict the gauge configurations to the so-called Gribov region (or more precisely, the fundamental modular region) where the Faddeev-Popov operator is positive. Because of the entropy considerations [20], a typical gauge configuration lies near the Gribov horizon where the lowest eigenvalue of the FP operator vanishes. Consequently, the ghost propagator and the color-Coulomb potential which contains the inverse of the FP operator twice become infrared singular. Recent lattice QCD simulations have revealed that the eigenmodes of the FP operator accumulate in the low-lying level and its density increases with increasing the lattice volume [6, 21].

In this study, we investigate the impact of the low-lying eigenmodes of the FP operator on the confining behavior of the color-Coulomb potential. The Gribov copy effects are taken into account by generating the gauge copies and by selecting the representatives that give the smallest value of the minimizing functional. We exploit the spectral representation of the FP ghost Green's function. Because the color-Coulomb potential can be expressed in terms of

the Green's function of the FP operator, the color-Coulomb potential is explicitly written as a spectral sum of the FP ghost eigenmodes. We examine how the long-distance behavior of the color-Coulomb potential is governed by the low-lying FP eigenmodes.

The organization of the paper is as follows. In the next section we express the color-Coulomb potential as the spectral sum of FP ghost eigenmodes. Section III is devoted to explain the technical details of the simulations and to show the results of our numerical simulations. The effects of the Gribov copies on the FP eigenvalues are examined in Sec. III A. In Sec. III B, the lowest FP eigenvalue will be shown to vanish in the infinite volume limit faster than that in the Landau gauge. The color-Coulomb potential obtained by the partial spectral sum and the color-Coulomb string tension are given in Secs. III C and III D. We will see that the low-lying modes account for the large portion of the color-Coulomb string tension, and the lowest eigenmode has a substantial contribution to the spectral sum. The results for the weight factor which controls the contribution of each eigenmode to the spectral sum are given in Sec. III E. The correlation function of the FP eigenmodes which is responsible for the distance dependence of each eigenmode is examined in Sec. III F. Finally, we present conclusions in Sec. IV.

II. SPECTRAL SUM FOR THE COLOR-COULOMB POTENTIAL

In the Coulomb gauge, the Hamiltonian can be decomposed into the transverse part and the instantaneous part [22];

$$\begin{aligned} H &= \frac{1}{2}\int d^3x \left\{ (E_i^{\rm tr})^2 + B_i^2 \right\} \\ &+ \frac{1}{2}\int d^3y \int d^3z \rho^a(\vec{y},t)\mathcal{V}^{ab}(\vec{y},\vec{z};A^{\rm tr})\rho^b(\vec{z},t). \end{aligned} \tag{1}$$

E_i are the transverse components of the color-electric field and $B_i^a \equiv \epsilon_{ijk}F_{jk}/2$ the color-magnetic fields. ρ is the color charge density

$$\rho^a = g f^{abc} A_i^{b,{\rm tr}} E_i^{c,{\rm tr}} + \rho^a_{\rm quark}. \tag{2}$$

Color charges interact with each other instantaneously through the kernel $\mathcal{V}$ which is expressed in terms of the Green's function M^{-1} of the FP ghost operator $M^{ab} = -\partial_i D_i^{ab} = -\delta^{ab}\partial_i^2 - g f^{abc} A_i^{c,{\rm tr}}\partial_i$,

$$\mathcal{V}^{ab}(\vec{y},\vec{z};A^{\rm tr}) = (M^{-1}[A](-\partial_i^2)M^{-1}[A])^{ab}_{\vec{y},\vec{z}}. \tag{3}$$

In the Abelian theory the FP operator is the negative Laplacian since the structure constants f^{abc} are zero. Accordingly the instantaneous interaction is reduced to the well-known Coulomb potential.

As can be seen from the Coulomb gauge Hamiltonian, the instantaneous interaction between quarks is proportional to the product of the color charges as the one-gluon exchange; namely, the instantaneous interaction is purely a two-body interaction and is proportional to the quadratic color factor [23]. The vacuum expectation value of the instantaneous interaction energy between a quark and an antiquark located at $\vec{x}$ and $\vec{y}$ is given by

$$V_c(\vec{x}-\vec{y}) = g^2 \vec{T}_q^a \cdot \vec{T}_{\bar{q}}^b \langle \mathcal{V}^{ab}(\vec{x},\vec{y};A^{\rm tr})\rangle, \tag{4}$$

and we call V_c the color-Coulomb potential. Here $\langle\cdot\rangle$ denotes the Monte Carlo average and $T^a_{q(\bar{q})}$ are the generators of the color-$SU(3)$ group. In the color-singlet channel the color-Coulomb potential is

$$V_c^{\rm singlet}(\vec{x}-\vec{y}) = g^2 \frac{-C_f}{N_c^2-1}\langle \mathcal{V}^{aa}(\vec{x},\vec{y};A^{\rm tr})\rangle, \tag{5}$$

where $C_f = 4/3$ is the Casimir invariant in the fundamental representation of the color-$SU(3)$ group and $-C_f$ is the color factor in the singlet channel. N_c is the number of colors. In this paper we are interested in only the color-singlet channel and for simplicity we denote the color-Coulomb potential in the singlet channel by V_c.

Our definition of the color-Coulomb potential is slightly different from what appeared in [22] where the color-Coulomb potential is given as the instantaneous part of the time-time component of the gluon propagator,

$$\begin{aligned} D_{44}(x-y) &= {\rm Tr}\langle A_4(\vec{x},x_4)A_4(\vec{y},y_4)\rangle \\ &= V_c'(|\vec{x}-\vec{y}|)\delta(x_4-y_4) + P(x-y). \end{aligned} \tag{6}$$

V_c' can be written as

$$V_c'(|\vec{x}-\vec{y}|)\delta^{ab} = g^2\langle \mathcal{V}^{ab}(\vec{x},\vec{y};A^{\rm tr})\rangle. \tag{7}$$

Therefore, our definition of the color-Coulomb potential differs from that in [22] by the color factor $-C_f$.

The Green's function of the FP operator can be expanded explicitly in terms of the eigenfunctions ϕ_n and the eigenvalues λ_n of the FP operator as

$$(M^{-1}[A])^{ab}(\vec{x},\vec{y}) = \sum_n \frac{\phi_n^{*a}(\vec{x})\phi_n^b(\vec{y})}{\lambda_n}, \tag{8}$$

where the sum extends over the whole eigenmodes besides the trivial zero modes.

In the same way, the color-Coulomb potential can be written as a spectral sum of the ghost eigenmodes,

$$V_c(\vec{x}-\vec{y}) = g^2\frac{-C_f}{N_c^2-1}\left\langle \sum_{n,m}\phi_n^{*a}(\vec{x})\phi_m^a(\vec{y})\frac{\int d^3z\phi_n^c(\vec{z})(-\partial_i^2)\phi_m^{*c}(\vec{z})}{\lambda_n\lambda_m}\right\rangle. \tag{9}$$

We notice that the distance dependence of the color-Coulomb potential comes from the product of the eigenmodes $\phi_n^{*a}(\vec{x})\phi_m^b(\vec{y})$. The remaining part,

$$\omega_{nm} = \frac{\int d^3z\phi_n^c(\vec{z})(-\partial_i^2)\phi_m^{*c}(\vec{z})}{\lambda_n\lambda_m}, \tag{10}$$

gives a weight of the contributions from each eigenmode. In the Abelian theory, the eigenvalue is $1/\vec{p}^2$ and the eigenfunctions are the plane waves since the FP operator is the negative Laplacian. Therefore the weight factor becomes diagonal and is proportional to the inverse of the FP eigenvalue, $\omega_{nm} \propto \delta_{nm}/\lambda_n$.

In the Gribov-Zwanziger scenario the FP eigenmodes get accumulated in the low-lying modes [20], and as the volume increases the lowest eigenvalue of the FP operator in the Yang-Mills theory goes toward zero faster than that in the Abelian theory where the lowest eigenvalue of the FP operator on a lattice is $4\sin^2(\pi/L)$, see Sec. III B. Accordingly we expect that the lowest component of the weight factor ω_{11} becomes significantly large in the Yang-Mills theory and the color-Coulomb potential is dominated by the lowest FP eigenmode.

III. NUMERICAL SIMULATIONS

The lattice configurations $U = \{U_\mu(x)\}$ are generated by the Cabibbo-Marinari pseudo-heat-bath algorithm [24] with the Wilson plaquette action on several lattice volumes and lattice couplings. Ten thousand sweeps are discarded for thermalization and a measurement has been done every 100 sweeps. The lattice parameters used in this study are summarized in Table I.

The Coulomb gauge condition

$$\partial_i A_i(\vec{x},t) = 0 \tag{11}$$

does not mix the spatial components and the temporal component of the gauge fields, and each time slice is gauge-fixed independently. In this work, we adopt the Wilson-Mandula iterative method with the Fourier acceleration to fix to the Coulomb gauge [25]; namely, we minimize the functional

$$F_U[g] = \frac{1}{L^3}\sum_{\vec{x}}\mathfrak{Re}\,\mathrm{Tr}\left(1-\frac{1}{3}g^\dagger(\vec{x},t)U_\mu(\vec{x},t)g(\vec{x}+\vec{i},t)\right) \tag{12}$$

with respect to the gauge transformation $g(\vec{x},t)\in SU(3)$ and find the local minimum of $F_U[g]$. Here L^3 is the spatial lattice volume. The gauge fields $A_\mu(\vec{x},t)$ are defined as

$$A_\mu(\vec{x},t) = \left.\frac{U_\mu(\vec{x},t)-U_\mu^\dagger(\vec{x},t)}{2iag_0}\right|_{\rm traceless}, \tag{13}$$

and the gauge fields at the minima of $F_U[g]$ satisfy the transversality condition $\nabla_i A_i(\vec{x},t)=0$ where ∇ is the lattice backward difference. We stop the iterative gauge fixing if the violation of the transversality becomes less than 10^{-14};

$$\theta = \frac{1}{(N_c^2-1)L^3}\sum_{a,\vec{x}}(\nabla_i A_i^a(\vec{x},t))^2 < 10^{-14}. \tag{14}$$

This stopping criterion is applied for each time slice. We refer the configurations gauge-fixed in this way to *first copies*.

In order to examine the effects of Gribov copies, we generate 30 gauge copies by performing the random gauge transformation for each time slice. Then, we find the minimum of the functional (12). Configurations giving a lowest value of the minimizing functional among the gauge copies for all time slices are called *best copies*, candidates of gauge configurations in the fundamental modular region. In this way, we can prepare the configurations that are close to the fundamental modular region and discuss the Gribov copy effects.

The effects of the Gribov copies on the color-Coulomb potential obtained by inverting the FP operator in the conjugate gradient method have been discussed in [26]. It has been clarified that the Gribov copies tremendously affect the color-Coulomb potential at small momenta. In the following, we shall see that the color-Coulomb string tension extracted from the spectral sum of the FP eigenmodes is also influenced by the Gribov copies.

TABLE I: The lattice couplings, the lattice volumes, the number of configurations used to evaluate the FP eigenvalues and the corresponding eigenfunctions. N_{cp} refers to the number of random gauge copies generated for each time slice to investigate the Gribov copy effects.

β	L^4	a^{-1} [GeV]	a [fm]	V[fm^4]	# of confs.	N_{cp}
5.70	8^4	1.160	0.1702	1.36^4	100	30
	16^4	1.160	0.1702	2.72^4	100	30
5.80	8^4	1.446	0.1364	1.09^4	100	30
	12^4	1.446	0.1364	1.64^4	100	30
	16^4	1.446	0.1364	2.18^4	100	30
	20^4	1.446	0.1364	2.73^4	100	30
	24^4	1.446	0.1364	3.27^4	100	30
6.00	8^4	2.118	0.0931	0.74^4	100	30
	16^4	2.118	0.0931	1.49^4	100	30
	24^4	2.118	0.0931	2.23^4	100	30
6.20	8^4	2.914	0.0677	0.54^4	100	30
	16^4	2.914	0.0677	1.08^4	100	30
	24^4	2.914	0.0677	1.63^4	100	30

In the Coulomb gauge the FP operator is a $8L^3\times 8L^3$ matrix on a lattice and a purely spatial quantity. It can be expressed in terms of the spatial link variables $U_i(x)$ as

$$M^{ab}_{\vec{x}\vec{y}} = \sum_i \mathfrak{Re}\mathrm{Tr}\left[\{T^a,T^b\}\left(U_i(\vec{x},t)+U_i(\vec{x}-\hat{i},t)\right)\delta_{\vec{x},\vec{y}} - 2T^bT^aU_i(\vec{x},t)\delta_{\vec{y},\vec{x}+\hat{i}} - 2T^aT^bU_i(\vec{x}-\hat{i})\delta_{\vec{y},\vec{x}-\hat{i}}\right]. \tag{15}$$

Since the FP matrix is the Hessian matrix associated with the functional (12), the eigenvalues we obtain are positive. In $SU(3)$ Yang-Mills theory there are eight trivial zero modes associated with the spatially constant eigenfunctions. We exclude these modes from the spectral sum of the color-Coulomb potential.

We solve the eigenvalue equation

$$M\phi_n = \lambda_n\phi_n, \tag{16}$$

and evaluate low-lying 300 eigenvalues and the corresponding eigenvectors including the trivial zero modes using the ARPACK package [27]. The spectral representation of the color-Coulomb potential in the singlet channel is

$$V_c(R) = g^2\frac{-C_f}{N_c^2-1}\left\langle \sum_{k,l=n_{\min}}^{n_{\max}} \phi_k^{*a}(\vec{x})\phi_l^a(\vec{y})\omega_{kl}\right\rangle, \tag{17}$$

where $R=|\vec{x}-\vec{y}|$. We investigate the behavior of the color-Coulomb potential by changing the lower and the upper limits of the spectral sum, $n_{\min}$ and $n_{\max}$. Statistical errors are estimated by the jackknife method.

A. Effects of the Gribov copies on the FP eigenvalues

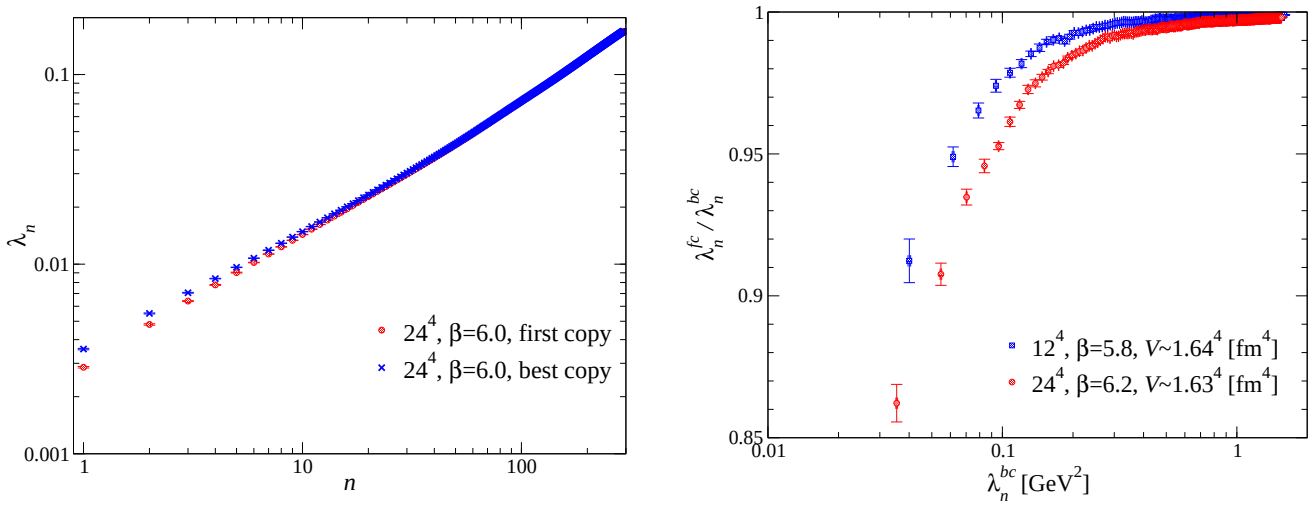

FIG. 1: (Left) The eigenvalues of the FP operator on the 24^4 lattice at $\beta = 6.0$ for the first copies and the best copies. (Right) The ratio $\lambda_n^{fc}/\lambda_n^{bc}$ of the FP eigenvalues on almost the same physical volume is plotted as a function of λ_n^{bc}.

We discuss the effects of the Gribov copies on the eigenvalues of the FP operator. In the left panel of Fig. 1, the lowest nontrivial 292 eigenvalues evaluated on the first copies and the best copies on the 24^4 lattice at $\beta = 6.0$ are plotted. We observe that the first copies underestimate the FP eigenvalues and the discrepancies are large at small eigenvalues. The ratio $\lambda_n^{fc}/\lambda_n^{bc}$ of the FP eigenvalues on almost the same physical volume is plotted in the right panel of Fig. 1. Here λ_n^{fc} refers to the FP eigenvalue for the first copies and λ_n^{bc} for the best copies. We see that the ratio decreases as we get close to the critical limit (i.e., the thermodynamic limit and the continuum limit). The effects of the Gribov copies cause more than 10 % systematic errors for the lowest eigenvalue on the 24^4 lattice. This indicates that we have to pay adequate attention to the Gribov copy effects on the FP eigenvalues.

The reason why the best copies give larger eigenvalues than the first copies can be explained as follows. Except for the trivial zero modes, the FP eigenvalues are strictly positive for the trivial vacuum $A = 0$. As we come close to the first Gribov horizon, the lowest eigenvalue decreases and becomes zero for configurations on the first Gribov horizon. The fundamental modular region is a subset of the Gribov region and its boundary does not necessarily coincide with the Gribov horizon, although it has a common boundary with the Gribov region [20]. Therefore, the fundamental modular region has a small overlap with the Gribov horizon compared to the Gribov region. It implies that the FP eigenvalues for the best copies are larger than that for the first copies, which is seen in our result.

B. Lowest eigenvalues of the FP operator

At the zeroth order of the coupling, the FP operator is the negative Laplacian, $M^{ab} = -\delta^{ab}\partial_i^2$, and there are $(N_c^2 - 1)$ nontrivial lowest eigenmodes taking the value

$$\lambda = \left[\frac{2}{a}\sin\left(\frac{\pi}{L}\right)\right]^2, \tag{18}$$

which are degenerated. In the infinite volume limit, this eigenvalue approaches zero as

$$\left[\frac{2}{a}\sin\left(\frac{\pi}{L}\right)\right]^2 \longrightarrow \left(\frac{1}{aL}\right)^2. \tag{19}$$

We investigate the volume dependence of the lowest eigenvalues of the FP operator and see if they vanish faster than that for the negative Laplacian, Eq. (19).

In Fig. 2, the lowest eigenvalues, λ_i $(i = 1, 2, 5, 8)$, for the best copies are plotted as a function of the inverse of the spatial extent of the lattice. We find that the eigenvalues decrease with increasing the lattice volumes. Moreover,

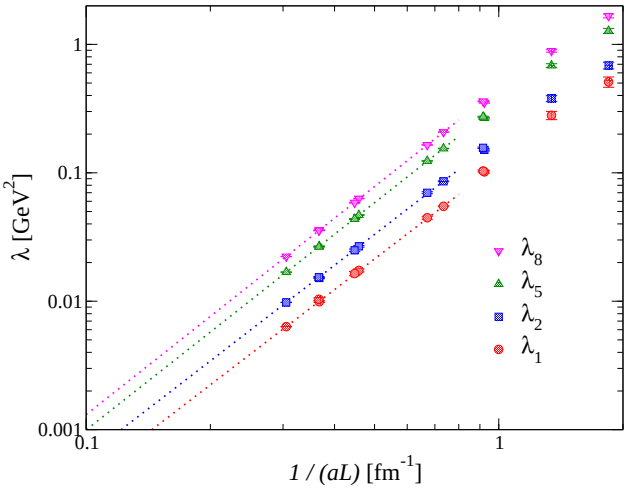

FIG. 2: The lowest eigenvalues, λ_i $(i = 1, 2, 5, 8)$, for the best copies are plotted as a function of the inverse of the spatial lattice extent. The dotted lines correspond to the fitted results.

TABLE II: The fitted results for the lowest eigenvalues of the FP operator. $(1/aL)_{\rm max}$ [fm^{-1}] is the maximum value of the fitting range.

λ_i	$(1/aL)_{\rm max}$ [fm^{-1}]	b	c	$\chi^2/N_{\rm DF}$
λ_1	0.6	0.121(6)	2.49(4)	1.02
	0.7	0.121(4)	2.48(3)	0.77
	0.8	0.118(1)	2.46(1)	0.76
λ_2	0.6	0.180(6)	2.46(3)	0.67
	0.7	0.186(4)	2.48(2)	0.86
	0.8	0.185(2)	2.48(1)	0.72
λ_5	0.6	0.331(6)	2.51(2)	0.30
	0.7	0.339(3)	2.53(1)	0.74
	0.8	0.338(2)	2.53(1)	0.61
λ_8	0.6	0.461(6)	2.55(1)	1.17
	0.7	0.455(3)	2.54(1)	1.15
	0.8	0.454(2)	2.54(1)	0.93

the data points seem to lie on straight lines in the log-log plot. In order to explore the volume dependence of the eigenvalues, we fit the data with the function

$$\lambda_i = b \left(\frac{1}{aL} \right)^c , \tag{20}$$

in the range $(1/aL) \leq (1/aL)_{\rm max}$. The fitted parameters are given in Table II. The corresponding fitted functions for $(1/aL)_{\rm max} = 0.8$ [fm^{-1}] are drawn in Fig. 2 by the dotted lines. We observe that the fitting works well and the exponent c is larger than 2 in all the cases. It implies that not only the lowest FP eigenvalue approaches zero faster than that of the lattice Laplacian operator, but the low-lying eigenvalues also do. Our result is consistent with the hypothesis in the Gribov-Zwanziger scenario that the measure of the path integral is concentrated on the part of the horizon where "all horizons are one horizon" [28].

This has also been observed in the Landau gauge [29]. However, the fitting results have been obtained as 2.16(4), 2.24(5), and 2.45(4) for λ_1, λ_2, and λ_5, respectively. It means that the lowest eigenvalue of the FP operator in the Coulomb gauge vanishes faster than that in the Landau gauge. Since the ghost propagator can be expanded by the FP eigenmodes as Eq. (8), it may be expected to be enhanced in the Coulomb gauge compared to the Landau gauge.

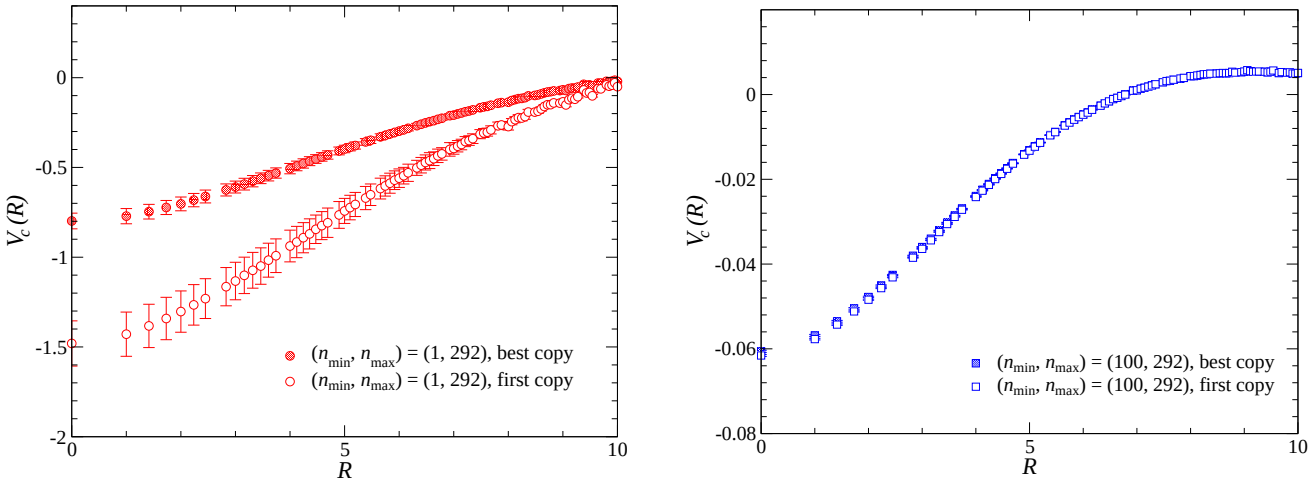

FIG. 3: The spectral sum of the color-Coulomb potential for the first and the best copies on the 24^4 lattice at $\beta = 6.0$ in lattice units. The lower-upper limit of the sum is $(1, 292)$ on the left figure and $(100, 292)$ on the right figure.

C. Spectral sum of the color-Coulomb potential

We here discuss the spectral sum of the color-Coulomb potential. Figure 3 illustrates the effects of Gribov copies on the color-Coulomb potential. In the left figure, the result for $(n_{\rm min}, n_{\rm max}) = (1, 292)$ is shown. We find that the color-Coulomb potential becomes shallow for the best copies compared to the first copy result. The discrepancy between the first and the best copies reaches about 200% at $R = 0$. In addition to the absolute value, the statistical errors are also influenced by the Gribov copies; namely, they are reduced for the best copies. Accordingly, it is indispensable to take into account the effects of the Gribov copies to calculate the color-Coulomb potential.

In the right panel of Fig. 3, the color-Coulomb potential for $(n_{\rm min}, n_{\rm max}) = (100, 292)$ is depicted. We see that the spectral sum of the color-Coulomb potential is less affected by the Gribov copies if we exclude the low-lying modes from the summation. This result is quite consistent with those discussed in the previous subsection, that is, the higher FP eigenvalues are less influenced by the Gribov copies.

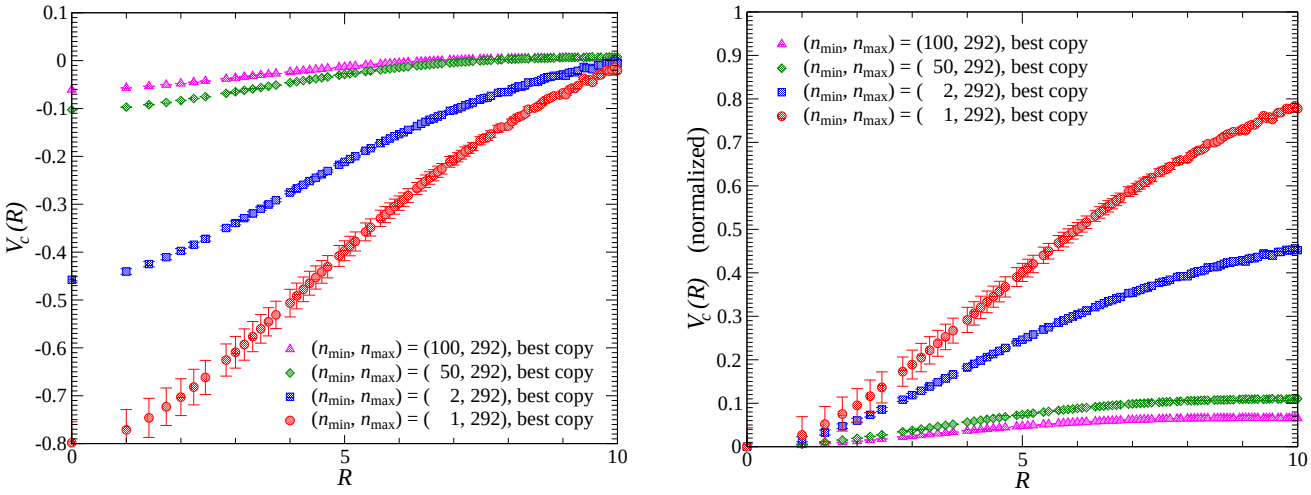

FIG. 4: (Left) The partially summed color-Coulomb potential as a function of R for the best copies in lattice units. Circles, squares, diamonds, and triangles correspond to $(n_{\rm min}, n_{\rm max}) = (1, 292), (2, 292), (50, 292), (100, 292)$, respectively. (Right) The partially summed color-Coulomb potential normalized to be 0 at $R = 0$ in order to make the distance dependence more visible.

The partial spectral sum of the color-Coulomb potential for the best copies is plotted in Fig. 4. The right panel illustrates the color-Coulomb potential normalized to be 0 at $R = 0$ in order to make the distance dependence more visible. By comparing data for $n_{\rm min} = 1$ with different $n_{\rm min}$, we observe that the exclusion of the near-zero modes substantially reduces the slope and the absolute value of the color-Coulomb potential. This is because the low-lying

components of the weight factor, ω_{nm}, are quite large and ω_{nm} rapidly decrease by increasing n or m, as we shall show later. We should mention that the long-distance behavior of the potential is governed by only a small fraction of ghost eigenmodes since the total number of the FP eigenvalues on the 24^4 lattice is $8L^3 = 110592$.

Data for $(n_{\min}, n_{\max}) = (50, 292)$ and $(100, 292)$ in Fig. 4 suggest that the inclusion of the eigenmodes in the range $50 \leq n \leq 99$ changes only the short-distance behavior of the color-Coulomb potential and the long-range part is not affected. From Fig. 4 we see that the absolute value of the color-Coulomb potential at large distances decreases by increasing $n_{\min}$ and it gets close to zero. In other words, the non low-lying modes contribute only to the short distant part of the potential and its long distant part is not altered by them. Thus the inclusion of the non low-lying FP eigenmodes changes only the short-distance behavior of the color-Coulomb potential.

D. Color-Coulomb string tension

TABLE III: The result of fitting the color-Coulomb potential with a straight line, $V(R) = K_c R + c$ in the range $4 \leq R \leq 7$. The Wilson string tension K_W is taken from [30].

$n_{\max}$	$K_c^{fc,\,\beta=6.0}$	$\chi^2/N_{\rm DF}$	$K_W^{\beta=6.0}$	K_c/K_W
1	0.1120(9)	0.19		2.18(12)
16	0.1490(12)	0.16		2.90(16)
30	0.1624(12)	0.19		3.17(18)
50	0.1668(12)	0.20	0.0513(25)	3.25(18)
100	0.1730(12)	0.23		3.37(19)
200	0.1782(12)	0.29		3.47(19)
292	0.1804(12)	0.36		3.52(19)

$n_{\max}$	$K_c^{bc,\,\beta=6.0}$	$\chi^2/N_{\rm DF}$	$K_W^{\beta=6.0}$	K_c/K_W
1	0.0413(22)	0.41		0.81(8)
8	0.0676(38)	0.26		1.32(14)
30	0.0798(37)	0.36		1.56(15)
50	0.0841(37)	0.38	0.0513(25)	1.64(15)
100	0.0901(37)	0.46		1.76(16)
200	0.0953(37)	0.78		1.86(16)
292	0.0975(37)	1.15		1.90(16)

$n_{\max}$	$K_c^{bc,\,\beta=5.8}$	$\chi^2/N_{\rm DF}$	$K_W^{\beta=5.8}$	K_c/K_W
1	0.1050(183)	0.08		0.96(19)
8	0.1249(65)	0.90		1.15(8)
30	0.1477(65)	1.13		1.36(8)
50	0.1550(65)	1.18	0.1090(20)	1.43(9)
100	0.1646(65)	1.28		1.51(9)
200	0.1720(65)	1.65		1.58(9)
292	0.1749(65)	2.08		1.60(9)

$n_{\max}$	$K_c^{bc,\,\beta=6.2}$	$\chi^2/N_{\rm DF}$	$K_W^{\beta=6.2}$	K_c/K_W
1	0.0276(24)	0.21		1.05(12)
8	0.0389(14)	1.92		1.48(9)
30	0.0469(14)	2.23		1.79(9)
50	0.0498(14)	2.03	0.0262(06)	1.90(10)
100	0.0544(14)	1.35		2.08(10)
200	0.0587(14)	1.46		2.24(10)
292	0.0609(14)	2.56		2.32(11)

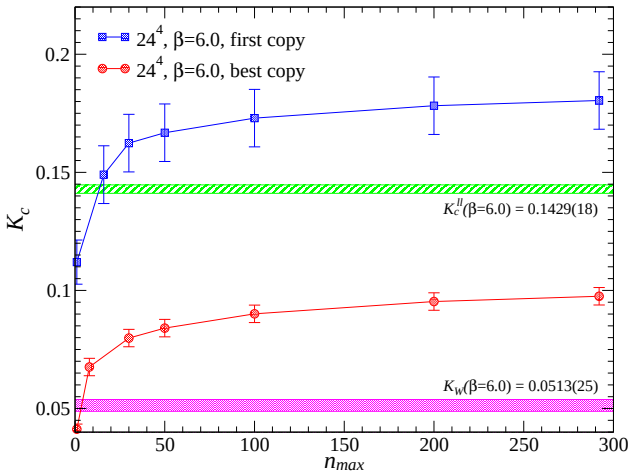

FIG. 5: The color-Coulomb string tension extracted by fitting the color-Coulomb potential with a straight line is plotted as a function of $n_{\max}$, the maximum FP mode in the spectral summation. The squares correspond to the first copy result on the 24^4 lattice at $\beta = 6.0$, and the circles represent the best copy one. The upper band and lower band indicate the color-Coulomb string tension K_c obtained by measuring the link-link correlator and the Wilson string tension K_W obtained from the Wilson loop calculation, respectively.

In order to reveal how the low-lying FP modes saturate the color-Coulomb potential at large distances, we extract the color-Coulomb string tension by fitting the potential with a straight line and investigate how the color-Coulomb string tension changes by varying the maximum mode $n_{\max}$ of the spectral sum. We do not include the Coulomb term, $1/r$, in the fitting function since the higher FP modes that are responsible for the short distant part of the color-Coulomb potential are not incorporated in the analysis. The fitted results are summarized in Table III. In this analysis, $n_{\min}$ is fixed to be 1. Thus, the result for $n_{\max} = 50$ means that the color-Coulomb potential is reconstructed from the low-lying 50 eigenmodes.

We discuss the effects of the Gribov copies on the color-Coulomb string tension. This is illustrated in Fig. 5, where the first copy and the best copy results are shown. The string tension K_c^{ll} of the color-Coulomb potential which is obtained by measuring the link-link correlator [1] and the Wilson string tension K_W, the string tension of the static potential, are also depicted by bands, respectively. We note that K_c^{ll} is the best copy result and the detail of the calculation is given in the Appendix. We find that the first copy result for K_c overestimates K_c^{ll} and it is more than 3 times larger than the Wilson string tension. By taking into account the Gribov copies, the color-Coulomb string tension is drastically reduced and it becomes less than K_c^{ll} although it is still larger than the Wilson string tension.

It may be not a problem that K_c does not agree with K_c^{ll}. The color-Coulomb potential can be calculated in different ways. One way is to calculate the color-Coulomb potential directly by inverting the FP matrix or solving the eigenvalue equation of the FP ghost matrix. In this method, only the spatial link variables at a fixed time slice are needed to calculate the color-Coulomb potential. The other way is to exploit the fact that the color-Coulomb potential is the instantaneous part of the time-time component of the gluon propagator,

$$D_{44}(\vec{x}, t) = V_c'(\vec{x})\delta(t) + P(\vec{x}, t), \tag{21}$$

and to calculate the correlator of the timelike links at a fixed time slice. Only the temporal links are needed to calculate the color-Coulomb potential in this method. Although these two ways provide a complementary way to obtain the color-Coulomb potential, the lattice results performed at finite lattice spacings do not necessarily agree. Of course, the results should c

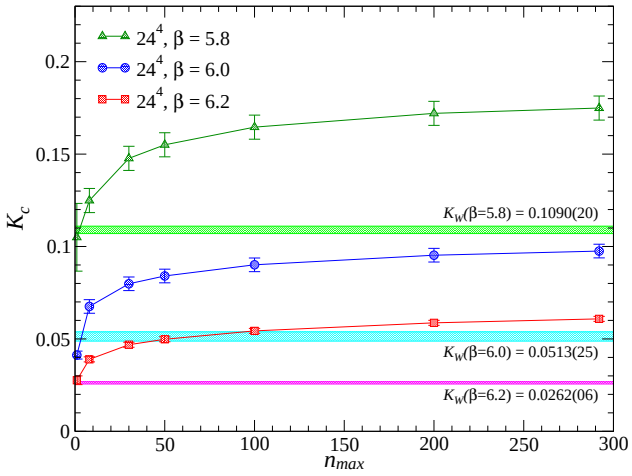

FIG. 6: The color-Coulomb string tension for the best copies is plotted as a function of $n_{\max}$, the maximum FP mode in the spectral summation. The Wilson string tension is also shown by the bands.

We next discuss the $n_{\max}$ dependence of the color-Coulomb string tension. The color-Coulomb string tension for the best copies at various lattice couplings and the corresponding Wilson string tension are displayed in Fig. 6. We see that the color-Coulomb string tension for the lowest eigenmode is comparable to the Wilson string tension, indicating that the lowest mode accounts for the large portion of the string tension. K_c rapidly increases at small $n_{\max}$, and the rate of increase decreases with $n_{\max}$. The values of K_c for $n_{\max} = 200$ and for $n_{\max} = 292$ almost agree within the statistical errors. Thus, it is expected that the further inclusion of the higher eigenmodes into the spectral sum does

[1] In this section, the color-Coulomb string tension for the spectral summed potential is referred to as K_c and the string tension of the color-Coulomb potential obtained from the link-link correlator is referred to as K_c^{ll}.

not alter the color-Coulomb string tension and the long-range behavior of the color-Coulomb potential is governed by the low-lying eigenmodes.

The ratio of the color-Coulomb string tension to the Wilson string tension is listed in Table III. We observe that the ratio for $n_{\max} = 292$ increases with increasing the lattice couplings, ranging from 1.6 to 2.3. Since the inclusion of the higher eigenmodes, which we do not take into account, does not reduce the values of the string tension, our results exclude the possibility that the color-Coulomb string tension saturates the Wilson string tension. Instead, the lowest FP eigenmode gives a large contribution to the color-Coulomb string tension comparable to the Wilson string tension.

In [5, 26], the color-Coulomb string tension has been estimated from the zero-momentum value of the color-Coulomb potential in momentum space. This method requires simulations on large lattice volumes to extract a reliable value of the string tension. However, large lattice simulations of the color-Coulomb potential are extremely cumbersome since we have to take into account the Gribov copies, which greatly influence the color-Coulomb potential. The method we used in this paper is superior in this respect; namely, the spectral expansion of the color-Coulomb potential in position space does not require so much large lattices and only a few hundreds of FP eigenmodes are needed to estimate the color-Coulomb string tension.

The fact that the color-Coulomb string tension is larger than the Wilson string tension is physically admissible. If K_c saturates K_W, the color-Coulomb potential has the same energy as the ground state energy of the QCD Hamiltonian, that is, the Wilson static potential. Since the color-Coulomb potential is the energy of the system obtained by adding a $q\bar{q}$ pair to the QCD vacuum [16], $K_c = K_W$ would indicate that such a state is also the eigenstate of the QCD Hamiltonian. The QCD vacuum does not have a flux tube, and it also holds for the state, $|\text{QCD vacuum} + q\bar{q} \text{ pair}\rangle$. Hence there is no room for the formation of the flux tube between quarks if K_c saturates K_W. Moreover, if such a state having no flux tube was the eigenstate of the QCD Hamiltonian, it could be found by the lattice calculations as the degenerated ground state of the $q\bar{q}$ system. Currently, the lattice simulations, however, suggest that the state with the flux tube is the ground state of the $q\bar{q}$ system and the state without the flux tube has not been found as the ground state of the QCD Hamiltonian. Thus, our result that the color-Coulomb string tension is larger than the Wilson string tension is quite reasonable.

E. Weight factor ω_{nm}

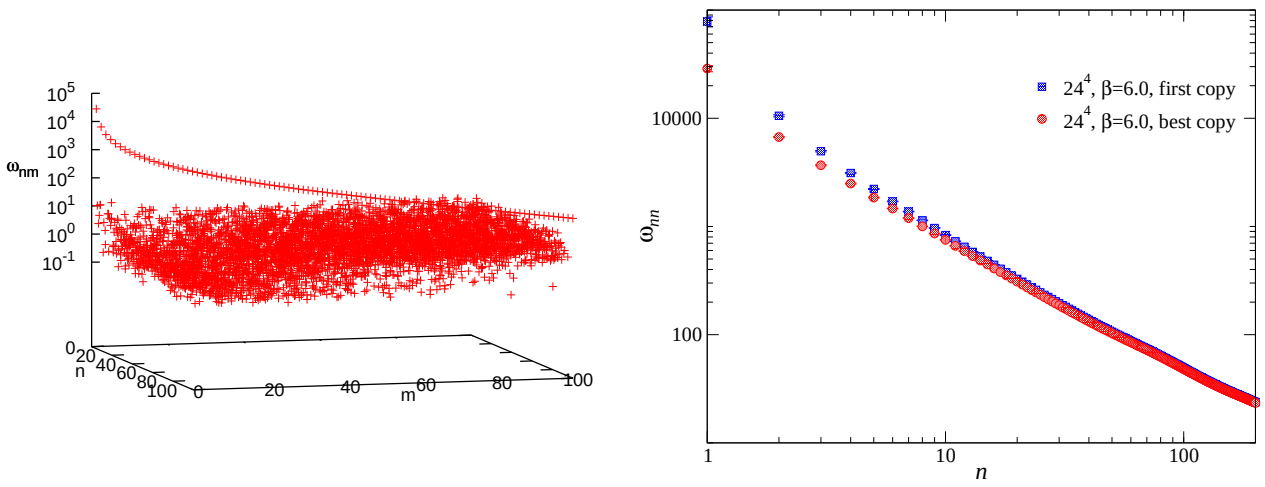

FIG. 7: (Left) ω_{nm} for the best copies are plotted as a function of n and m in the range $n, m = 1 \sim 100$. Statistical errors are not shown. (Right) The diagonal components of the weight factor, ω_{nn}, are plotted as a function of the label n in the range $1 \leq n \leq 200$ for both the first copy and the best copy results.

The weight factor ω_{nm} for the best copies is depicted in the left panel of Fig. 7. We observe that the diagonal components are extremely larger than the off-diagonal components. This means that the contributions to the spectral sum of the color-Coulomb potential from the combinations $\phi_n^*(\vec{x})\phi_m(\vec{y})$ with different eigenmodes $n \neq m$ are small. In the Abelian theory the off-diagonal components are exactly zero, $\omega_{nm} \sim \delta_{nm}/\lambda_n$. It is due to the non-Abelian nature of Yang-Mills theory that the off-diagonal components have finite values, even though they are quite small

compared to the diagonal components.

The diagonal components of the weight factor, ω_{nn}, are shown in the right panel of Fig. 7. In the figure, both the best copy and the first copy results are drawn. We find that the Gribov copy effects can be seen at small n and the two curves approach each other as n increases. For the lowest component ω_{11}, the ratio of the first copy result to the best copy one is about 2.7, that is, the systematic errors due to the Gribov copies reach 170%.

Figure 7 shows that the lowest component ω_{11} takes a significantly large value. For instance, ω_{22} is about 1/4 of ω_{11}, and the diagonal component for $n = 20$ is smaller than ω_{11} by a factor about 100. It implies that the lowest ghost eigenmode dominates the color-Coulomb potential. In the Gribov-Zwanziger scenario, a typical configuration lies near the Gribov horizon and the lowest FP eigenvalue goes to zero faster than the free field case as the lattice volume increases. Since the weight factor ω_{nm} contains the inverse of the FP eigenvalue twice, it is the expected result that the lowest component ω_{11} takes a significantly large value and the lowest FP eigenmode dominates the spectral sum of the color-Coulomb potential.

F. Correlation of the FP eigenmodes

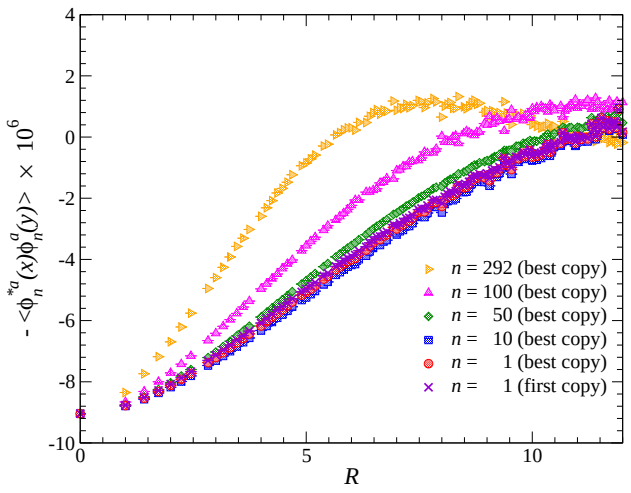

FIG. 8: The correlation function of the FP ghost eigenfunctions, $-\langle\phi_n^{*a}(\vec{x})\phi_n^a(\vec{y})\rangle$, is shown as a function of $R = |\vec{x} - \vec{y}|$.

The correlation function of the FP ghost eigenmodes, $-\langle\phi_n^{*a}(\vec{x})\phi_n^a(\vec{y})\rangle$, is shown in Fig. 8 as a function of $R = |\vec{x}-\vec{y}|$. As we have mentioned in Sec. II, the distance dependence of the color-Coulomb potential comes from the correlation function. We see that the correlation function of the low-lying FP eigenfunctions shows a linearly rising behavior. The distance dependence of the correlation function does not so much differ for $n \leq 50$. The confining behavior of the color-Coulomb potential is ascribed to the fact that the correlation function of the low-lying modes rises linearly and the corresponding w_{nm} take large values. Furthermore, we observe that the correlation function for $n = 292$ starts to decrease at a large distance; namely, the correlation function completely loses the confining property in the sense that it does not rise with distance. This result strongly supports our expectation that the higher eigenmodes that are not taken into account in our analysis do not change the long-range behavior of the color-Coulomb potential and the color-Coulomb string tension is almost saturated by the low-lying eigenmodes.

In addition to the distance dependence, we notice that the correlation function is not sensitive to the Gribov copy effects. This can be seen in Fig. 8 where the first copy and the best copy results are shown by red circles and violet crosses, respectively. Therefore, the Gribov copy effects on the color-Coulomb potential stem from that on the FP eigenvalues and the weight factor.

IV. SUMMARY

In this paper we discussed the effects of the Gribov copies on the FP eigenvalues and the essential role of the low-lying FP eigenmodes on the confining color-Coulomb potential in $SU(3)$ Coulomb gauge Yang-Mills theory using lattice Monte Carlo simulations.

The low-lying FP eigenvalues are sensitive to the Gribov copies and the discrepancy between the first copy and the best copy results exceeds 10% for the lowest eigenvalue. The volume scaling of the low-lying eigenvalues was investigated and we found that the lowest eigenvalue approaches zero much faster than that in the Landau gauge.

We exploited the fact that the color-Coulomb potential can be expressed as the spectral sum of the FP ghost eigenmodes. It was shown that the long-distance linearity of the color-Coulomb potential is ascribed to the low-lying FP eigenmodes. Changing $n_{\max}$ does not alter the color-Coulomb string tension for $n_{\max} \geq 200$ within the statistical errors, and about 300 eigenmodes almost saturate the string tension. The ratio of the color-Coulomb potential to the Wilson string tension takes values raging from 1.6 to 2.3. This is consistent with the Zwanziger's inequality. Moreover, the contribution of the lowest eigenmode to the string tension is comparable to the Wilson string tension. Since the inclusion of the higher eigenmodes that have not been taken into account does not reduce the string tension, our estimated values of the string tension give a lower limit for the color-Coulomb string tension. Thus, our result excludes the possibility that the color-Coulomb string tension saturates the Wilson string tension.

We observed that the weight factor is also sensitive to the Gribov copies. The systematic errors on the lowest component due to the copies are shown to be about 170%. Although the Gribov copy effects are large, the lowest component takes a quite large value compared to the higher components. This leads to the fact that the lowest eigenmode has a substantial contribution to the spectral sum of the color-Coulomb potential.

The correlation function of the FP eigenfunctions is shown to be insensitive to the Gribov copies. Accordingly, the Gribov copy effects on the color-Coulomb potential stem from that on the FP eigenvalues. The correlation function of the low-lying eigenmodes increases with the distance. By contrast, the correlation function for $n = 292$ decreases at large distances. Therefore, such eigenmodes do not account for the confining property of the color-Coulomb potential. This supports our finding that the color-Coulomb string tension is not altered so much by including the eigenmodes higher than $n \sim 200$. Our results strongly support the Gribov-Zwanziger scenario: The infrared dynamics of Yang-Mills theory is governed by the configurations near the Gribov horizon where the lowest eigenvalue vanishes.

V. ACKNOWLEDGMENTS

The simulation was performed on NEC SX-8R at RCNP, and NEC SX-9 at CMC, Osaka University. We appreciate the warm hospitality and support of the RCNP administrators. Y. N. is supported by a JSPS Grant-in-Aid from the Ministry of Education, Culture, Sports, Science and Technology of Japan. The work is partially supported by a Grant-in-Aid for Scientific Research by Monbu-kagakusyo, No. 20340055.

Appendix A: Link-link correlator and the Color-Coulomb potential

In this Appendix, we present the best copy results for the color-Coulomb potential in the color-singlet channel obtained by measuring the correlator of the temporal links. The necessary equations can be found in [15, 17, 23], and various parameters of the gauge configurations are given in Table IV.

TABLE IV: The lattice couplings, the lattice volumes, the number of configurations used to calculate the color-Coulomb potential. N_{cp} refers to the number of random gauge copies generated for each time slice to investigate the Gribov copy effects.

β	L^4	a^{-1} [GeV]	a [fm]	V[fm^4]	# of confs.	N_{cp}
6.00	12^4	2.118	0.0931	1.12^4	100	30
6.00	16^4	2.118	0.0931	1.49^4	100	30
6.00	20^4	2.118	0.0931	1.86^4	100	30
6.00	24^4	2.118	0.0931	2.23^4	100	30

The left panel of Fig. 9 shows the color-Coulomb potential for the best and the first copies on the 24^4 lattice at $\beta = 6.0$, and the right panel illustrates the ratio V_c^{fc}/V_c^{bc} of the color-Coulomb potential as a function of the distance on various lattice sizes at $\beta = 6.0$. V_c^{fc} refers to the color-Coulomb potential for the first copies and V_c^{bc} for the best copies. We see that the first copies overestimate the color-Coulomb potential. The deviation is a few percent while the effects of Gribov copies increase with distance. The ratio V_c^{fc}/V_c^{bc} decreases with increasing the lattice volume up to the 20^4 lattice, although we do not see such a tendency on the 24^4 lattice. It should be noted that the Gribov copy effects are milder than those on the color-Coulomb potential obtained by the spectral sum of the FP eigenmodes or by inverting the FP operator. Further studies are requisite to elucidate why the FP eigenvalues are tremendously affected by the Gribov copies but the correlator of the temporal links are not.

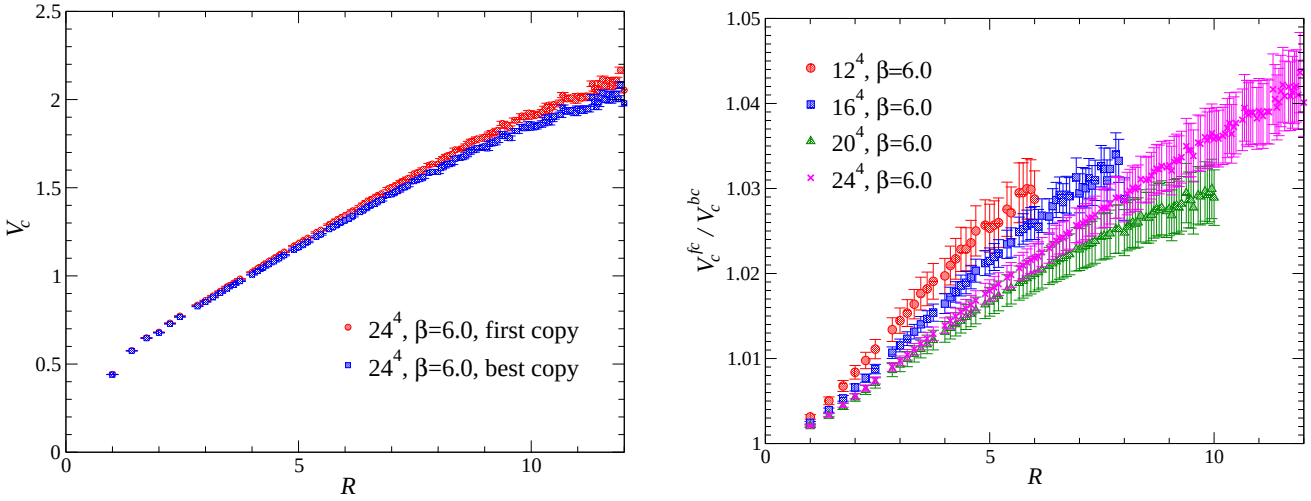

FIG. 9: (Left) The color-Coulomb potential in the color-singlet channel on the 24^4 lattice at $\beta = 6.0$ for the first copies and the best copies. (Right) The ratio V_c^{fc}/V_c^{bc} of the color-Coulomb potential on various lattice sizes at $\beta = 6.0$.

We perform a two-parameter fit to extract the string tension of the color-Coulomb potential,

$$V_c(R) = c + K_c R - \frac{\pi}{12R}, \tag{A1}$$

in the range $4 \le R \le 7$ and find

$$c = 0.502(6), \quad K_c = 0.1429(18), \quad \chi^2/N_{\rm DF} = 0.082. \tag{A2}$$

The fitting without the Lüscher term, $-\pi/12R$, gives

$$c = 0.399(5), \quad K_c = 0.1527(17), \quad \chi^2/N_{\rm DF} = 0.146. \tag{A3}$$

The color-Coulomb string tension is about 3 times larger than the Wilson string tension, $K_W = a^2\sigma_W = 0.0513(25)$ [30], in agreement with the fact that the color-Coulomb potential provides an upper bound for the static Wilson potential.

[1] J. Greensite, Prog. Part. Nucl. Phys. **51**, 1 (2003), [hep-lat/0301023].
[2] D. Zwanziger, Prog. Theor. Phys. Suppl. **131**, 233 (1998), [hep-th/9802180].
[3] A. Cucchieri, AIP Conf. Proc. **892**, 22 (2007), [hep-lat/0612004].
[4] A. Cucchieri and D. Zwanziger, Phys. Rev. **D65**, 014001 (2001), [hep-lat/0008026].
[5] K. Langfeld and L. Moyaerts, Phys. Rev. **D70**, 074507 (2004), [hep-lat/0406024].
[6] Y. Nakagawa, A. Nakamura, T. Saito and H. Toki, Phys. Rev. **D75**, 014508 (2007), [hep-lat/0702002].
[7] M. Quandt, G. Burgio, S. Chimchinda and H. Reinhardt, PoS **LAT2007**, 325 (2007), [0710.0549].
[8] A. Voigt, E.-M. Ilgenfritz, M. Muller-Preussker and A. Sternbeck, PoS **LAT2007**, 338 (2007), [0709.4585].
[9] Y. Nakagawa *et al.*, Phys. Rev. **D79**, 114504 (2009), [0902.4321].
[10] G. Burgio, M. Quandt and H. Reinhardt, Phys. Rev. Lett. **102**, 032002 (2009), [0807.3291].
[11] Y. Nakagawa, A. Nakamura, T. Saito and H. Toki, arXiv:0911.2550 [hep-lat].
[12] D. Zwanziger, Phys. Rev. D **69**, 016002 (2004).
[13] J. Greensite and S. Olejnik, Phys. Rev. **D67**, 094503 (2003), [hep-lat/0302018].
[14] J. Greensite, S. Olejnik and D. Zwanziger, Phys. Rev. **D69**, 074506 (2004), [hep-lat/0401003].
[15] A. Nakamura and T. Saito, Prog. Theor. Phys. **115**, 189 (2006), [hep-lat/0512042].
[16] D. Zwanziger, Phys. Rev. Lett. **90**, 102001 (2003), [hep-lat/0209105].
[17] Y. Nakagawa, A. Nakamura, T. Saito, H. Toki and D. Zwanziger, Phys. Rev. **D73**, 094504 (2006), [hep-lat/0603010].
[18] V. N. Gribov, Nucl. Phys. **B139**, 1 (1978).
[19] I. M. Singer, Commun. Math. Phys. **60**, 7 (1978).
[20] D. Zwanziger, Nucl. Phys. **B412**, 657 (1994).
[21] J. Greensite, S. Olejnik and D. Zwanziger, JHEP **05**, 070 (2005), [hep-lat/0407032].

[22] A. Cucchieri and D. Zwanziger, Phys. Rev. **D65**, 014002 (2001), [hep-th/0008248].
[23] Y. Nakagawa, A. Nakamura, T. Saito and H. Toki, Phys. Rev. **D77**, 034015 (2008), [arXiv:0802.0239 [hep-lat]].
[24] N. Cabibbo and E. Marinari, Phys. Lett. **B119**, 387 (1982).
[25] C. T. H. Davies *et al.*, Phys. Rev. **D37**, 1581 (1988).
[26] A. Voigt, E. M. Ilgenfritz, M. Muller-Preussker and A. Sternbeck, Phys. Rev. **D78**, 014501 (2008), [0803.2307].
[27] http://www.caam.rice.edu/software/arpack/.
[28] D. Zwanziger, Nucl. Phys. **B399**, 477 (1993).
[29] A. Sternbeck, E. M. Ilgenfritz and M. Muller-Preussker, Phys. Rev. **D73**, 014502 (2006), [hep-lat/0510109].
[30] G. S. Bali and K. Schilling, Phys. Rev. **D47**, 661 (1993), [hep-lat/9208028].